Relaxed linearized algorithms for faster X-ray CT image reconstruction

Hung Nien and Jeffrey A. Fessler

University of Michigan, Ann Arbor

The 13th Fully 3D Meeting – June 2, 2015

Statistical image reconstruction for X-ray CT

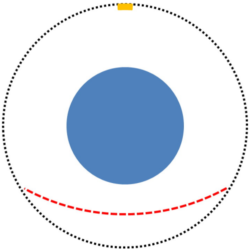

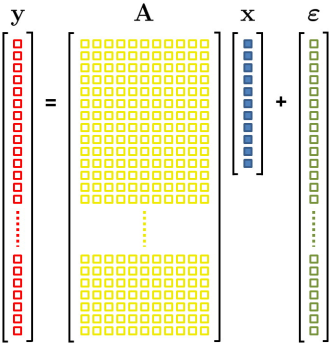

Statistical image reconstruction for X-ray CT

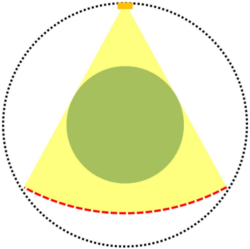

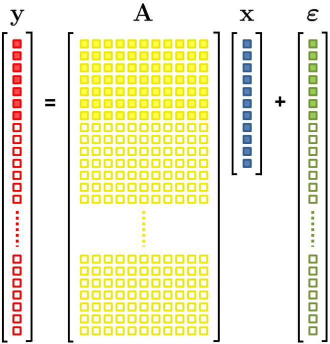

Statistical image reconstruction for X-ray CT

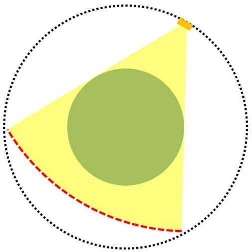

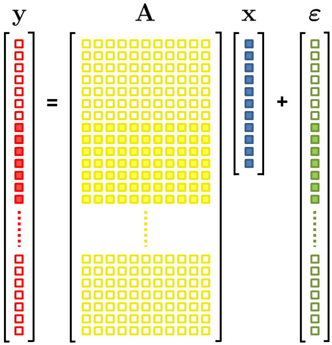

Statistical image reconstruction for X-ray CT

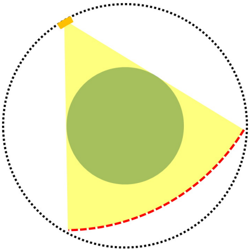

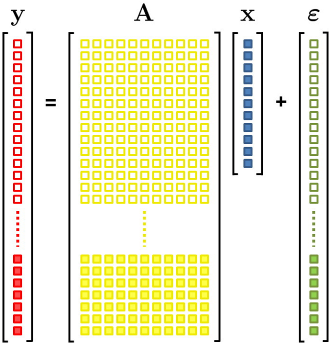

Statistical image reconstruction for X-ray CT

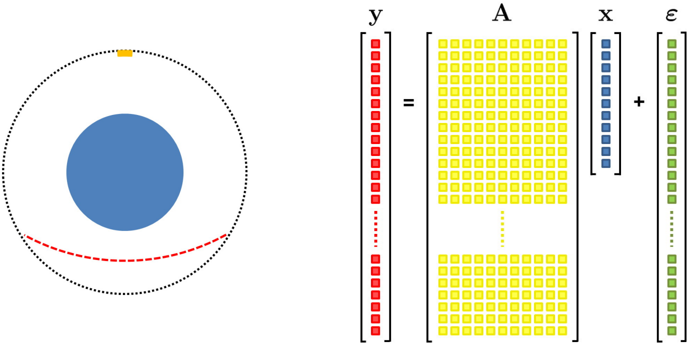

Statistical image reconstruction for X-ray CT

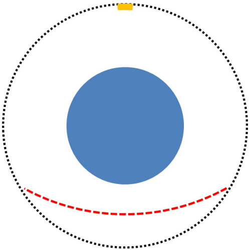

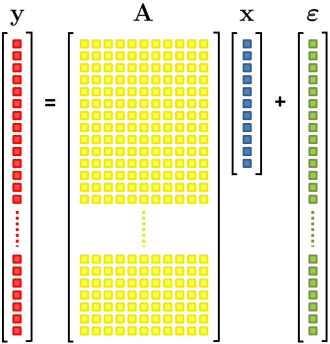

Statistical image reconstruction (SIR)

$$\hat{\mathbf{x}} \in \arg\min_{\mathbf{x}} \left\{ \Psi_{\text{PWLS}}(\mathbf{x}) \triangleq \frac{1}{2} \|\mathbf{y} - \mathbf{A}\mathbf{x}\|_{\mathbf{W}}^2 + \mathsf{R}(\mathbf{x}) + \iota_{\Omega}(\mathbf{x}) \right\}$$

Statistical image reconstruction for X-ray CT

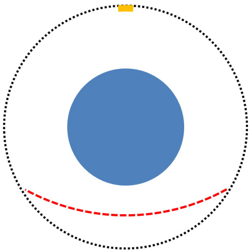

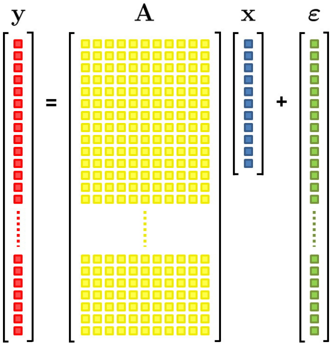

Statistical image reconstruction (SIR)

$$\hat{\mathbf{x}} \in \arg\min_{\mathbf{x}} \left\{ \Psi_{\mathrm{PWLS}}(\mathbf{x}) \triangleq \frac{1}{2} \|\mathbf{y} - \mathbf{A}\mathbf{x}\|^2_{\mathbf{W}} + \mathrm{R}(\mathbf{x}) + \iota_{\Omega}(\mathbf{x}) \right\}$$

Statistical image reconstruction for X-ray CT

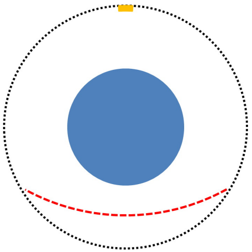

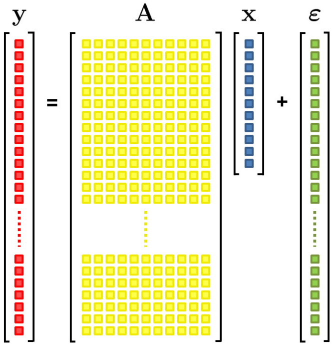

Statistical image reconstruction (SIR)

$$\hat{\mathbf{x}} \in \arg\min_{\mathbf{x}} \left\{ \Psi_{\mathrm{PWLS}}(\mathbf{x}) \triangleq \frac{1}{2} \|\mathbf{y} - \mathbf{A}\mathbf{x}\|_{\mathbf{W}}^2 + \mathsf{R}(\mathbf{x}) + \iota_{\Omega}(\mathbf{x}) \right\}$$

Statistical image reconstruction for X-ray CT

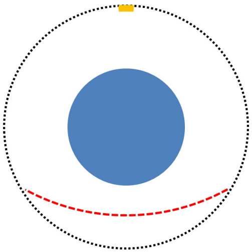

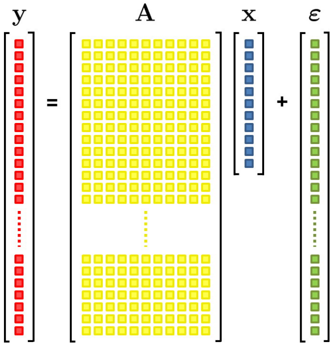

Statistical image reconstruction (SIR)

$$\hat{\mathbf{x}} \in \arg\min_{\mathbf{x}} \left\{ \Psi_{\mathrm{PWLS}}(\mathbf{x}) \triangleq \frac{1}{2} \|\mathbf{y} - \mathbf{A}\mathbf{x}\|_{\mathbf{W}}^2 + \mathrm{R}(\mathbf{x}) + \iota_{\Omega}(\mathbf{x}) \right\}$$

Statistical image reconstruction for X-ray CT

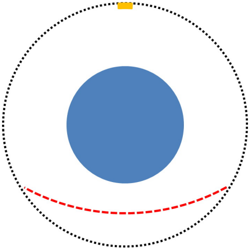

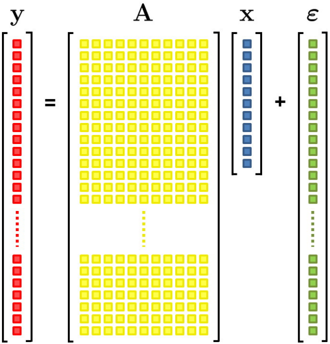

Statistical image reconstruction (SIR)

$$\hat{\mathbf{x}} \in \arg\min_{\mathbf{x}} \left\{ \Psi_{\mathrm{PWLS}}(\mathbf{x}) \triangleq \frac{1}{2} \|\mathbf{y} - \mathbf{A}\mathbf{x}\|_{\mathbf{W}}^2 + \mathrm{R}(\mathbf{x}) + \iota_{\Omega}(\mathbf{x}) \right\}$$

First-order algorithms with ordered-subsets

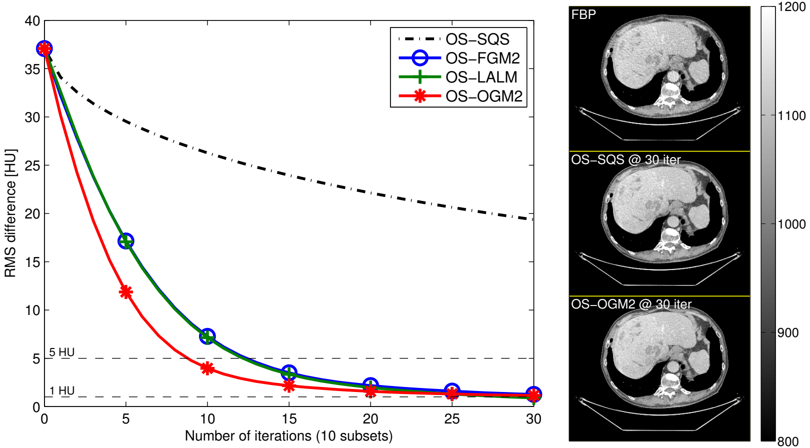

Figure: Chest: Existing first-order algorithms with ordered-subsets (OS).

COLLEGE OF ENGINEERING
ELECTRICAL ENGINEERING & COMPUTER SCIENCE
UNIVERSITY OF MICHIGAN

First-order algorithms with ordered-subsets

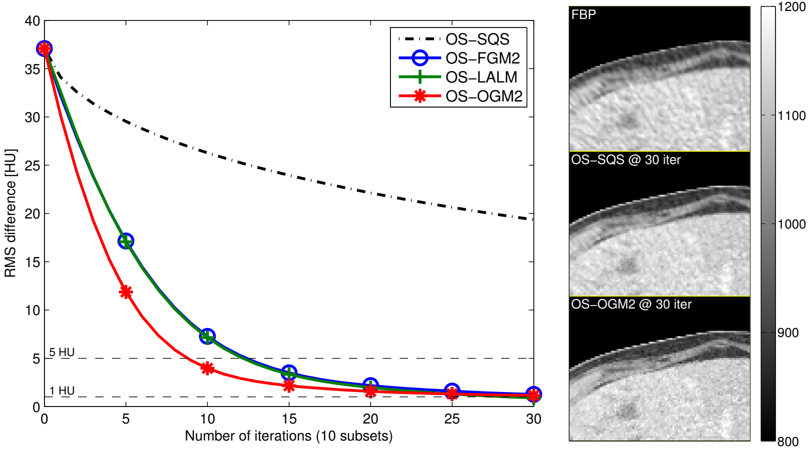

Figure: Chest: Existing first-order algorithms with ordered-subsets (OS).

First-order algorithms with ordered-subsets

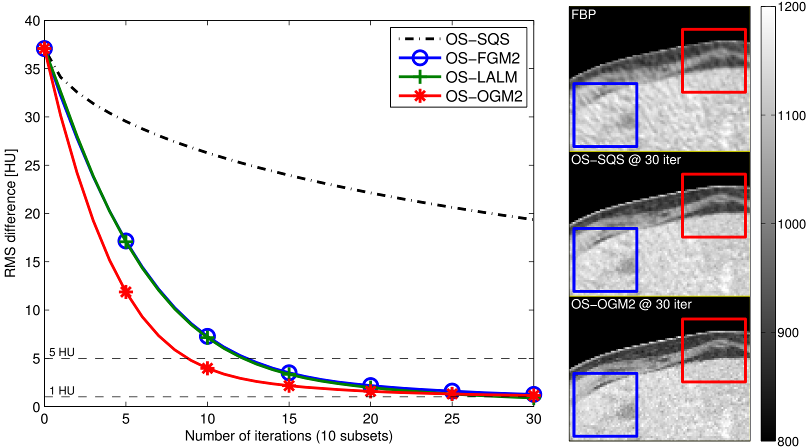

Figure: Chest: Existing first-order algorithms with ordered-subsets (OS).

First-order algorithms with ordered-subsets

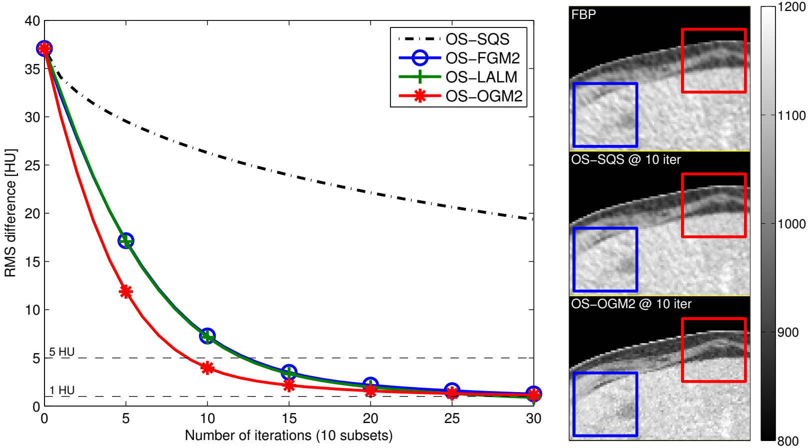

Figure: Chest: Existing first-order algorithms with ordered-subsets (OS).

First-order algorithms with ordered-subsets

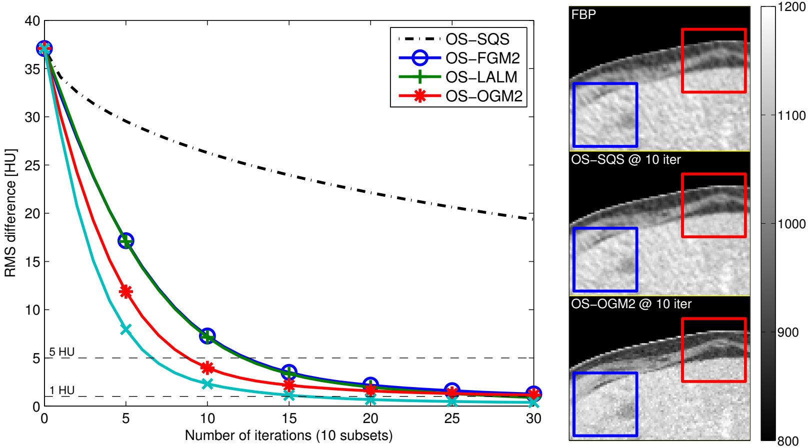

Figure: Chest: Existing first-order algorithms with ordered-subsets (OS).

Equality-constrained composite minimization

Consider an equality-constrained minimization problem:

$$(\hat{\mathbf{x}}, \hat{\mathbf{u}}) \in \arg\min_{\mathbf{x},\mathbf{u}} \left\{ \frac{1}{2} \|\mathbf{u} - \mathbf{y}\|_2^2 + h(\mathbf{x}) \right\} \text{ s.t. } \mathbf{u} = \mathbf{A}\mathbf{x}\,, \qquad (1)$$

where h are closed and proper convex functions.

Equality-constrained composite minimization

Consider an equality-constrained minimization problem:

$$(\hat{\mathbf{x}}, \hat{\mathbf{u}}) \in \arg\min_{\mathbf{x},\mathbf{u}} \left\{ \frac{1}{2} \|\mathbf{u} - \mathbf{y}\|_2^2 + h(\mathbf{x}) \right\} \text{ s.t. } \mathbf{u} = \mathbf{A}\mathbf{x}\,, \tag{1}$$

where h are closed and proper convex functions.

In particular, the quadratic loss function penalizes the difference between the linear model $\mathbf{A}\mathbf{x}$ and noisy measurement $\mathbf{y}$, and h is a regularization term that introduces the prior knowledge of $\mathbf{x}$ to the reconstruction.

Equality-constrained composite minimization

Consider an equality-constrained minimization problem:

$$(\hat{\mathbf{x}}, \hat{\mathbf{u}}) \in \arg\min_{\mathbf{x},\mathbf{u}} \left\{ \frac{1}{2} \|\mathbf{u} - \mathbf{y}\|_2^2 + h(\mathbf{x}) \right\} \text{ s.t. } \mathbf{u} = \mathbf{A}\mathbf{x}\,, \tag{1}$$

where h are closed and proper convex functions.

In particular, the quadratic loss function penalizes the difference between the linear model $\mathbf{A}\mathbf{x}$ and noisy measurement $\mathbf{y}$, and h is a regularization term that introduces the prior knowledge of $\mathbf{x}$ to the reconstruction. For example,

$$(\hat{\mathbf{x}}, \hat{\mathbf{u}}) \in \arg\min_{\mathbf{x},\mathbf{u}} \left\{ \frac{1}{2} \left\| \mathbf{u} - \mathbf{W}^{1/2}\mathbf{y} \right\|_2^2 + (\mathrm{R} + \iota_\Omega)(\mathbf{x}) \right\} \text{ s.t. } \mathbf{u} = \mathbf{W}^{1/2}\mathbf{A}\mathbf{x}$$

represents an X-ray CT image reconstruction problem.

Standard AL method

The standard AL method finds a saddle-point of the augmented Lagrangian (AL) of (1):

$$\mathcal{L}_{\mathsf{A}}(\mathbf{x}, \mathbf{u}, \mathbf{d}; \rho) \triangleq \frac{1}{2} \|\mathbf{u} - \mathbf{y}\|_2^2 + h(\mathbf{x}) + \frac{\rho}{2} \|\mathbf{A}\mathbf{x} - \mathbf{u} - \mathbf{d}\|_2^2$$

in an alternating direction manner:

$$\begin{cases} \mathbf{x}^{(k+1)} \in \arg\min_{\mathbf{x}} \left\{ h(\mathbf{x}) + \frac{\rho}{2} \left\| \mathbf{A}\mathbf{x} - \mathbf{u}^{(k)} - \mathbf{d}^{(k)} \right\|_2^2 \right\} \\ \mathbf{u}^{(k+1)} \in \arg\min_{\mathbf{u}} \left\{ \frac{1}{2} \|\mathbf{u} - \mathbf{y}\|_2^2 + \frac{\rho}{2} \left\| \mathbf{A}\mathbf{x}^{(k+1)} - \mathbf{u} - \mathbf{d}^{(k)} \right\|_2^2 \right\} \\ \mathbf{d}^{(k+1)} = \mathbf{d}^{(k)} - \mathbf{A}\mathbf{x}^{(k+1)} + \mathbf{u}^{(k+1)}, \end{cases}$$

where $\mathbf{d}$ is the scaled Lagrange multiplier of $\mathbf{u}$, and $\rho > 0$ is the AL penalty parameter.

[Gabay and Mercier, Comput. Math. Appl., 1976]

Standard AL method

The standard AL method finds a saddle-point of the augmented Lagrangian (AL) of (1):

$$\mathcal{L}_{\mathsf{A}}(\mathbf{x}, \mathbf{u}, \mathbf{d}; \rho) \triangleq \frac{1}{2}\|\mathbf{u}-\mathbf{y}\|_2^2 + h(\mathbf{x}) + \frac{\rho}{2}\|\mathbf{A}\mathbf{x}-\mathbf{u}-\mathbf{d}\|_2^2$$

in an alternating direction manner:

$$\begin{cases} \mathbf{x}^{(k+1)} \in \arg\min_{\mathbf{x}} \left\{ h(\mathbf{x}) + \frac{\rho}{2}\left\|\mathbf{A}\mathbf{x}-\mathbf{u}^{(k)}-\mathbf{d}^{(k)}\right\|_2^2 \right\} \\ \mathbf{u}^{(k+1)} \in \arg\min_{\mathbf{u}} \left\{ \frac{1}{2}\|\mathbf{u}-\mathbf{y}\|_2^2 + \frac{\rho}{2}\left\|\mathbf{A}\mathbf{x}^{(k+1)}-\mathbf{u}-\mathbf{d}^{(k)}\right\|_2^2 \right\} \\ \mathbf{d}^{(k+1)} = \mathbf{d}^{(k)} - \mathbf{A}\mathbf{x}^{(k+1)} + \mathbf{u}^{(k+1)}, \end{cases}$$

where $\mathbf{d}$ is the scaled Lagrange multiplier of $\mathbf{u}$, and $\rho > 0$ is the AL penalty parameter.

[Gabay and Mercier, Comput. Math. Appl., 1976]

Linearized AL method

The linearized AL method adds an additional **G**-proximity term to the **x**-subproblem in the standard AL method:

$$\begin{cases} \mathbf{x}^{(k+1)} \in \arg\min_{\mathbf{x}} \left\{ h(\mathbf{x}) + \frac{\rho}{2} \left\| \mathbf{A}\mathbf{x} - \mathbf{u}^{(k)} - \mathbf{d}^{(k)} \right\|_2^2 + \frac{\rho}{2} \left\| \mathbf{x} - \mathbf{x}^{(k)} \right\|_{\mathbf{G}}^2 \right\} \\ \mathbf{u}^{(k+1)} \in \arg\min_{\mathbf{u}} \left\{ \frac{1}{2} \left\| \mathbf{u} - \mathbf{y} \right\|_2^2 + \frac{\rho}{2} \left\| \mathbf{A}\mathbf{x}^{(k+1)} - \mathbf{u} - \mathbf{d}^{(k)} \right\|_2^2 \right\} \\ \mathbf{d}^{(k+1)} = \mathbf{d}^{(k)} - \mathbf{A}\mathbf{x}^{(k+1)} + \mathbf{u}^{(k+1)}, \end{cases}$$

where $\mathbf{G} \triangleq \mathbf{D}_{\mathsf{L}} - \mathbf{A}'\mathbf{A}$, and $\mathbf{D}_{\mathsf{L}}$ is a diagonal majorizing matrix of $\mathbf{A}'\mathbf{A}$.

[Zhang et al., J. Sci. Comput., 2011]
[HN and Fessler, IEEE Trans. Med. Imag., 2015]

Linearized AL method

The linearized AL method adds an additional **G**-proximity term to the **x**-subproblem in the standard AL method:

$$
\begin{cases}
\mathbf{x}^{(k+1)} \in \arg\min_{\mathbf{x}} \left\{ h(\mathbf{x}) + \frac{\rho}{2}\left\|\mathbf{A}\mathbf{x} - \mathbf{u}^{(k)} - \mathbf{d}^{(k)}\right\|_2^2 + \frac{\rho}{2}\left\|\mathbf{x} - \mathbf{x}^{(k)}\right\|_{\mathbf{G}}^2 \right\} \\
\mathbf{u}^{(k+1)} \in \arg\min_{\mathbf{u}} \left\{ \frac{1}{2}\left\|\mathbf{u} - \mathbf{y}\right\|_2^2 + \frac{\rho}{2}\left\|\mathbf{A}\mathbf{x}^{(k+1)} - \mathbf{u} - \mathbf{d}^{(k)}\right\|_2^2 \right\} \\
\mathbf{d}^{(k+1)} = \mathbf{d}^{(k)} - \mathbf{A}\mathbf{x}^{(k+1)} + \mathbf{u}^{(k+1)},
\end{cases}
$$

where $\mathbf{G} \triangleq \mathbf{D}_\mathsf{L} - \mathbf{A}'\mathbf{A}$, and $\mathbf{D}_\mathsf{L}$ is a diagonal majorizing matrix of $\mathbf{A}'\mathbf{A}$. Here, we linearize the algorithm in a sense that the Hessian matrix of the "augmented" quadratic AL term is diagonal.

[Zhang et al., J. Sci. Comput., 2011]
[HN and Fessler, IEEE Trans. Med. Imag., 2015]

Linearized AL algorithm for X-ray CT

Algorithm: OS-LALM for CT reconstruction.

Input: $K \geq 1$, $M \geq 1$, and an initial (FBP) image $\mathbf{x}$.

set $\rho = 1$, $\zeta = \mathbf{g} = M\nabla \mathsf{L}_M(\mathbf{x})$
for $k = 1, 2, \ldots, K$ **do**
  for $m = 1, 2, \ldots, M$ **do**
    $\mathbf{s} = \rho\zeta + (1-\rho)\,\mathbf{g}$
    $\mathbf{x}^+ = \left[\mathbf{x} - (\rho\mathbf{D}_\mathsf{L} + \mathbf{D}_\mathsf{R})^{-1}(\mathbf{s} + \nabla\mathsf{R}(\mathbf{x}))\right]_\Omega$
    $\zeta^+ = M\nabla\mathsf{L}_m(\mathbf{x}^+)$
    $\mathbf{g}^+ = \frac{\rho}{\rho+1}\zeta^+ + \frac{1}{\rho+1}\mathbf{g}$
    decrease ρ gradually
  end
end

Output: The final image $\mathbf{x}$.

Relaxed AL method

The relaxed AL method accelerates the standard AL method with under- or over-relaxation:

$$\begin{cases} \mathbf{x}^{(k+1)} \in \arg\min_{\mathbf{x}} \left\{ h(\mathbf{x}) + \frac{\rho}{2} \left\| \mathbf{A}\mathbf{x} - \mathbf{u}^{(k)} - \mathbf{d}^{(k)} \right\|_2^2 \right\} \\ \mathbf{u}^{(k+1)} \in \arg\min_{\mathbf{u}} \left\{ \frac{1}{2} \|\mathbf{u} - \mathbf{y}\|_2^2 + \frac{\rho}{2} \left\| \mathbf{r}_{\mathbf{u},\alpha}^{(k+1)} - \mathbf{u} - \mathbf{d}^{(k)} \right\|_2^2 \right\} \\ \mathbf{d}^{(k+1)} = \mathbf{d}^{(k)} - \mathbf{r}_{\mathbf{u},\alpha}^{(k+1)} + \mathbf{u}^{(k+1)} , \end{cases}$$

where

$$\mathbf{r}_{\mathbf{u},\alpha}^{(k+1)} \triangleq \alpha \mathbf{A}\mathbf{x}^{(k+1)} + (1-\alpha)\mathbf{u}^{(k)}$$

is the relaxation variable of $\mathbf{u}$, and $0 < \alpha < 2$ is the relaxation parameter.

[Eckstein and Bertsekas, Math. Prog., 1992]

Relaxed AL method

The relaxed AL method accelerates the standard AL method with under- or over-relaxation:

$$\begin{cases} \mathbf{x}^{(k+1)} \in \arg\min_{\mathbf{x}} \left\{ h(\mathbf{x}) + \frac{\rho}{2} \left\| \mathbf{A}\mathbf{x} - \mathbf{u}^{(k)} - \mathbf{d}^{(k)} \right\|_2^2 \right\} \\ \mathbf{u}^{(k+1)} \in \arg\min_{\mathbf{u}} \left\{ \frac{1}{2} \left\| \mathbf{u} - \mathbf{y} \right\|_2^2 + \frac{\rho}{2} \left\| \mathbf{r}_{\mathbf{u},\alpha}^{(k+1)} - \mathbf{u} - \mathbf{d}^{(k)} \right\|_2^2 \right\} \\ \mathbf{d}^{(k+1)} = \mathbf{d}^{(k)} - \mathbf{r}_{\mathbf{u},\alpha}^{(k+1)} + \mathbf{u}^{(k+1)}, \end{cases}$$

where

$$\mathbf{r}_{\mathbf{u},\alpha}^{(k+1)} \triangleq \alpha \mathbf{A}\mathbf{x}^{(k+1)} + (1-\alpha)\mathbf{u}^{(k)}$$

is the relaxation variable of $\mathbf{u}$, and $0 < \alpha < 2$ is the relaxation parameter. When $\alpha = 1$, it reverts to the standard AL method.

[Eckstein and Bertsekas, Math. Prog., 1992]

Implicit linearization via redundant variable-splitting

Consider an equivalent equality-constrained minimization problem with a redundant equality constraint:

$$(\hat{\mathbf{x}}, \hat{\mathbf{u}}, \hat{\mathbf{v}}) \in \arg\min_{\mathbf{x},\mathbf{u},\mathbf{v}} \left\{ \frac{1}{2} \|\mathbf{u} - \mathbf{y}\|_2^2 + h(\mathbf{x}) \right\} \text{ s.t. } \begin{cases} \mathbf{u} = \mathbf{A}\mathbf{x} \\ \mathbf{v} = \mathbf{G}^{1/2}\mathbf{x} \,. \end{cases}$$

[HN and Fessler, IEEE Trans. Med. Imag., 2015]

Implicit linearization via redundant variable-splitting

Consider an equivalent equality-constrained minimization problem with a redundant equality constraint:

$$(\hat{\mathbf{x}}, \hat{\mathbf{u}}, \hat{\mathbf{v}}) \in \arg\min_{\mathbf{x},\mathbf{u},\mathbf{v}} \left\{ \frac{1}{2} \|\mathbf{u} - \mathbf{y}\|_2^2 + h(\mathbf{x}) \right\} \text{ s.t. } \begin{cases} \mathbf{u} = \mathbf{A}\mathbf{x} \\ \mathbf{v} = \mathbf{G}^{1/2}\mathbf{x} \, . \end{cases}$$

Suppose we use the same AL penalty parameter ρ for both equality constraints in AL methods. The quadratic AL term

$$\frac{\rho}{2}\left\|\mathbf{A}\mathbf{x} - \mathbf{u}^{(k)} - \mathbf{d}^{(k)}\right\|_2^2 + \frac{\rho}{2}\left\|\mathbf{G}^{1/2}\mathbf{x} - \mathbf{v}^{(k)} - \mathbf{e}^{(k)}\right\|_2^2$$

has a diagonal Hessian matrix $\mathbf{H}_\rho \triangleq \rho\mathbf{A}'\mathbf{A} + \rho\mathbf{G} = \rho\mathbf{D}_\mathsf{L}$, leading to a separable quadratic AL term.

[HN and Fessler, IEEE Trans. Med. Imag., 2015]

Proposed relaxed linearized AL method

The proposed relaxed linearized AL method solves the equivalent minimization problem with a redundant equality constraint using the relaxed AL method:

$$\begin{cases} \mathbf{x}^{(k+1)} \in \arg\min_{\mathbf{x}} \left\{ \begin{aligned} & h(\mathbf{x}) + \frac{\rho}{2} \left\| \mathbf{A}\mathbf{x} - \mathbf{u}^{(k)} - \mathbf{d}^{(k)} \right\|_2^2 \\ & \quad + \frac{\rho}{2} \left\| \mathbf{G}^{1/2}\mathbf{x} - \mathbf{v}^{(k)} - \mathbf{e}^{(k)} \right\|_2^2 \end{aligned} \right\} \\ \mathbf{u}^{(k+1)} \in \arg\min_{\mathbf{u}} \left\{ \frac{1}{2} \left\| \mathbf{u} - \mathbf{y} \right\|_2^2 + \frac{\rho}{2} \left\| \mathbf{r}_{\mathbf{u},\alpha}^{(k+1)} - \mathbf{u} - \mathbf{d}^{(k)} \right\|_2^2 \right\} \\ \mathbf{d}^{(k+1)} = \mathbf{d}^{(k)} - \mathbf{r}_{\mathbf{u},\alpha}^{(k+1)} + \mathbf{u}^{(k+1)} \\ \mathbf{v}^{(k+1)} = \mathbf{r}_{\mathbf{v},\alpha}^{(k+1)} - \mathbf{e}^{(k)} \\ \mathbf{e}^{(k+1)} = \mathbf{e}^{(k)} - \mathbf{r}_{\mathbf{v},\alpha}^{(k+1)} + \mathbf{v}^{(k+1)} . \end{cases}$$

Proposed relaxed linearized AL method

The proposed relaxed linearized AL method solves the equivalent minimization problem with a redundant equality constraint using the relaxed AL method:

$$\begin{cases} \mathbf{x}^{(k+1)} \in \arg\min_{\mathbf{x}} \left\{ \begin{aligned} & h(\mathbf{x}) + \frac{\rho}{2}\left\|\mathbf{A}\mathbf{x} - \mathbf{u}^{(k)} - \mathbf{d}^{(k)}\right\|_2^2 \\ & \quad + \frac{\rho}{2}\left\|\mathbf{G}^{1/2}\mathbf{x} - \mathbf{v}^{(k)} - \mathbf{e}^{(k)}\right\|_2^2 \end{aligned} \right\} \\ \mathbf{u}^{(k+1)} \in \arg\min_{\mathbf{u}} \left\{ \frac{1}{2}\left\|\mathbf{u} - \mathbf{y}\right\|_2^2 + \frac{\rho}{2}\left\|\mathbf{r}_{\mathbf{u},\alpha}^{(k+1)} - \mathbf{u} - \mathbf{d}^{(k)}\right\|_2^2 \right\} \\ \mathbf{d}^{(k+1)} = \mathbf{d}^{(k)} - \mathbf{r}_{\mathbf{u},\alpha}^{(k+1)} + \mathbf{u}^{(k+1)} \\ \mathbf{v}^{(k+1)} = \mathbf{r}_{\mathbf{v},\alpha}^{(k+1)} - \mathbf{e}^{(k)} \\ \mathbf{e}^{(k+1)} = \mathbf{e}^{(k)} - \mathbf{r}_{\mathbf{v},\alpha}^{(k+1)} + \mathbf{v}^{(k+1)}. \end{cases}$$

When $\alpha = 1$, the proposed method reverts to the linearized AL method.

Proposed relaxed linearized AL method (cont'd)

The proposed relaxed linearized AL method further simplifies as follows:

$$\begin{cases} \gamma^{(k+1)} = (\rho - 1)\,\mathbf{g}^{(k)} + \rho \mathbf{h}^{(k)} \\ \mathbf{x}^{(k+1)} \in \arg\min_{\mathbf{x}} \left\{ h(\mathbf{x}) + \frac{1}{2} \left\| \mathbf{x} - (\rho \mathbf{D}_{\mathsf{L}})^{-1} \gamma^{(k+1)} \right\|^2_{\rho \mathbf{D}_{\mathsf{L}}} \right\} \\ \zeta^{(k+1)} = \nabla \mathsf{L}\left(\mathbf{x}^{(k+1)}\right) \triangleq \mathbf{A}' \left(\mathbf{A}\mathbf{x}^{(k+1)} - \mathbf{y}\right) \\ \mathbf{g}^{(k+1)} = \frac{\rho}{\rho+1}\left(\alpha \zeta^{(k+1)} + (1-\alpha)\mathbf{g}^{(k)}\right) + \frac{1}{\rho+1}\mathbf{g}^{(k)} \\ \mathbf{h}^{(k+1)} = \alpha\left(\mathbf{D}_{\mathsf{L}}\mathbf{x}^{(k+1)} - \zeta^{(k+1)}\right) + (1-\alpha)\mathbf{h}^{(k)}\,, \end{cases}$$

where $\mathsf{L}(\mathbf{x}) \triangleq (1/2)\,\|\mathbf{A}\mathbf{x} - \mathbf{y}\|_2^2$ denotes the quadratic data-fidelity term, and $\mathbf{g}^{(k)} \triangleq \mathbf{A}'\left(\mathbf{u}^{(k)} - \mathbf{y}\right)$ denotes the split gradient of L.

Proposed relaxed linearized AL method (cont'd)

The proposed relaxed linearized AL method further simplifies as follows:

$$\begin{cases} \gamma^{(k+1)} = (\rho - 1)\,\mathbf{g}^{(k)} + \rho\mathbf{h}^{(k)} \\ \mathbf{x}^{(k+1)} \in \arg\min_{\mathbf{x}} \left\{ h(\mathbf{x}) + \frac{1}{2}\left\|\mathbf{x} - (\rho\mathbf{D}_{\mathsf{L}})^{-1}\gamma^{(k+1)}\right\|_{\rho\mathbf{D}_{\mathsf{L}}}^2 \right\} \\ \zeta^{(k+1)} = \nabla\mathsf{L}\left(\mathbf{x}^{(k+1)}\right) \triangleq \mathbf{A}'\left(\mathbf{A}\mathbf{x}^{(k+1)} - \mathbf{y}\right) \\ \mathbf{g}^{(k+1)} = \frac{\rho}{\rho+1}\left(\alpha\zeta^{(k+1)} + (1-\alpha)\mathbf{g}^{(k)}\right) + \frac{1}{\rho+1}\mathbf{g}^{(k)} \\ \mathbf{h}^{(k+1)} = \alpha\left(\mathbf{D}_{\mathsf{L}}\mathbf{x}^{(k+1)} - \zeta^{(k+1)}\right) + (1-\alpha)\mathbf{h}^{(k)}, \end{cases}$$

where $\mathsf{L}(\mathbf{x}) \triangleq (1/2)\,\|\mathbf{A}\mathbf{x} - \mathbf{y}\|_2^2$ denotes the quadratic data-fidelity term, and $\mathbf{g}^{(k)} \triangleq \mathbf{A}'\left(\mathbf{u}^{(k)} - \mathbf{y}\right)$ denotes the split gradient of L.

Relaxed OS-LALM for faster CT reconstruction

To solve X-ray CT image reconstruction problem:

$$\hat{\mathbf{x}} \in \arg\min_{\mathbf{x}} \left\{ \frac{1}{2} \|\mathbf{y} - \mathbf{A}\mathbf{x}\|_{\mathbf{W}}^2 + \mathrm{R}(\mathbf{x}) + \iota_\Omega(\mathbf{x}) \right\}$$

using the proposed relaxed linearized AL method, we apply the following substitution:

$$\begin{cases} \mathbf{A} \leftarrow \mathbf{W}^{1/2}\mathbf{A} \\ \mathbf{y} \leftarrow \mathbf{W}^{1/2}\mathbf{y} \end{cases}$$

and set $h \triangleq \mathrm{R} + \iota_\Omega$.

Relaxed OS-LALM for faster CT reconstruction

To solve X-ray CT image reconstruction problem:

$$\hat{\mathbf{x}} \in \arg\min_{\mathbf{x}} \left\{ \frac{1}{2} \|\mathbf{y} - \mathbf{A}\mathbf{x}\|_{\mathbf{W}}^2 + \mathrm{R}(\mathbf{x}) + \iota_\Omega(\mathbf{x}) \right\}$$

using the proposed relaxed linearized AL method, we apply the following substitution:

$$\begin{cases} \mathbf{A} \leftarrow \mathbf{W}^{1/2}\mathbf{A} \\ \mathbf{y} \leftarrow \mathbf{W}^{1/2}\mathbf{y} \end{cases}$$

and set $h \triangleq \mathrm{R} + \iota_\Omega$.

The image update now is a diagonally weighted denoising problem. We solve it using a projected gradient descent step from $\mathbf{x}^{(k)}$.

Relaxed OS-LALM for faster CT reconstruction

To solve X-ray CT image reconstruction problem:

$$\hat{\mathbf{x}} \in \arg\min_{\mathbf{x}} \left\{ \frac{1}{2} \|\mathbf{y} - \mathbf{A}\mathbf{x}\|_{\mathbf{W}}^2 + \mathrm{R}(\mathbf{x}) + \iota_\Omega(\mathbf{x}) \right\}$$

using the proposed relaxed linearized AL method, we apply the following substitution:

$$\begin{cases} \mathbf{A} \leftarrow \mathbf{W}^{1/2}\mathbf{A} \\ \mathbf{y} \leftarrow \mathbf{W}^{1/2}\mathbf{y} \end{cases}$$

and set $h \triangleq \mathrm{R} + \iota_\Omega$.

The image update now is a diagonally weighted denoising problem. We solve it using a projected gradient descent step from $\mathbf{x}^{(k)}$. For speed-up, ordered subsets (OS) or incremental gradients are used.

Speed-up with decreasing continuation sequence

We also use a continuation technique to speed up convergence; that is, we decrease ρ gradually with iteration.

Speed-up with decreasing continuation sequence

We also use a continuation technique to speed up convergence; that is, we decrease ρ gradually with iteration.

Based on a second-order recursive system analysis, we use

$$\rho_i(\alpha) = \begin{cases} 1, & \text{if } i = 0 \\ \frac{\pi}{\alpha(i+1)}\sqrt{1 - \left(\frac{\pi}{2\alpha(i+1)}\right)^2}, & \text{otherwise}. \end{cases} \tag{2}$$

Therefore, we use a faster-decreasing continuation sequence in a more over-relaxed linearized AL method.

[HN and Fessler, IEEE Trans. Med. Imag., submitted]

Proposed relaxed linearized algorithm

Algorithm: Relaxed OS-LALM for CT reconstruction.

Input: $K \geq 1$, $M \geq 1$, $0 < \alpha < 2$, and an initial (FBP) image $\mathbf{x}$.

set $\rho = 1$, $\zeta = \mathbf{g} = M\nabla \mathsf{L}_M(\mathbf{x})$, $\mathbf{h} = \mathbf{D}_\mathsf{L}\mathbf{x} - \zeta$
for $k = 1, 2, \ldots, K$ **do**
  for $m = 1, 2, \ldots, M$ **do**

$$\mathbf{s} = \rho\left(\mathbf{D}_\mathsf{L}\mathbf{x} - \mathbf{h}\right) + (1-\rho)\,\mathbf{g}$$

$$\mathbf{x}^+ = \left[\mathbf{x} - \left(\rho\mathbf{D}_\mathsf{L} + \mathbf{D}_\mathsf{R}\right)^{-1}\left(\mathbf{s} + \nabla\mathsf{R}(\mathbf{x})\right)\right]_\Omega$$

$$\zeta = M\nabla\mathsf{L}_m(\mathbf{x}^+)$$

$$\mathbf{g}^+ = \tfrac{\rho}{\rho+1}\left(\alpha\zeta + (1-\alpha)\,\mathbf{g}\right) + \tfrac{1}{\rho+1}\mathbf{g}$$

$$\mathbf{h}^+ = \alpha\left(\mathbf{D}_\mathsf{L}\mathbf{x}^+ - \zeta\right) + (1-\alpha)\,\mathbf{h}$$

    decrease ρ using (2)
  end
end

Output: The final image $\mathbf{x}$.

Chest region helical scan

We reconstruct a $600 \times 600 \times 222$ image from an $888 \times 64 \times 3611$ helical (pitch 1.0) CT scan.

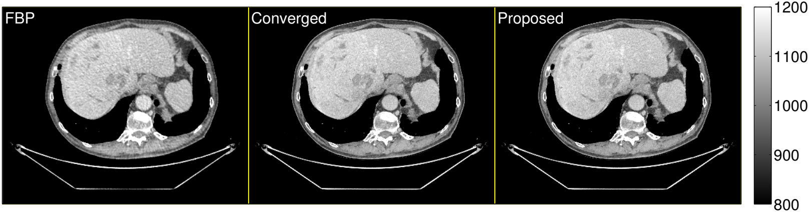

Figure: Chest: Cropped images of the initial FBP image $\mathbf{x}^{(0)}$ (left), the reference reconstruction $\mathbf{x}^{\star}$ (center), and the reconstructed image $\mathbf{x}^{(20)}$ using relaxed OS-LALM with 10 subsets after 20 iterations (right).

Chest region helical scan (cont'd)

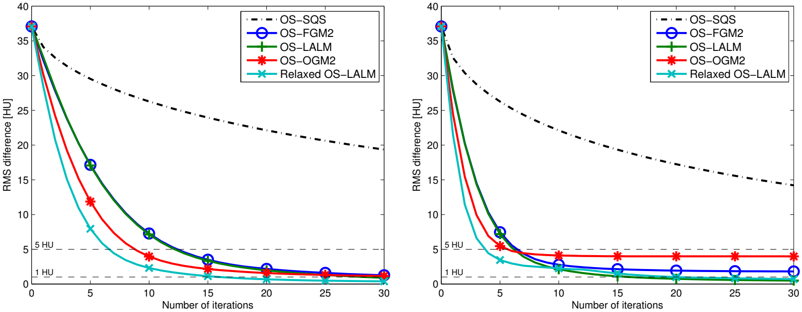

Figure: Chest: Convergence rate curves of different OS algorithms with 10 (left) and 20 (right) subsets.

Chest region helical scan (cont'd)

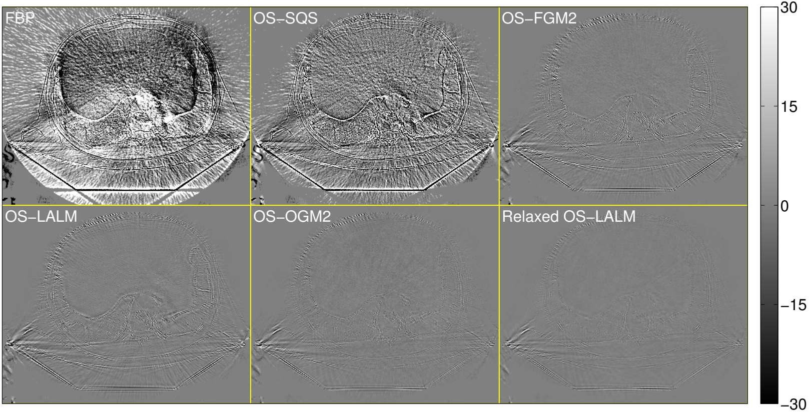

Figure: Chest: Difference images of the initial FBP image $\mathbf{x}^{(0)} - \mathbf{x}^{\star}$ and the reconstructed image $\mathbf{x}^{(10)} - \mathbf{x}^{\star}$ using OS algorithms with 10 subsets after 10 iterations.

Chest region helical scan (cont'd)

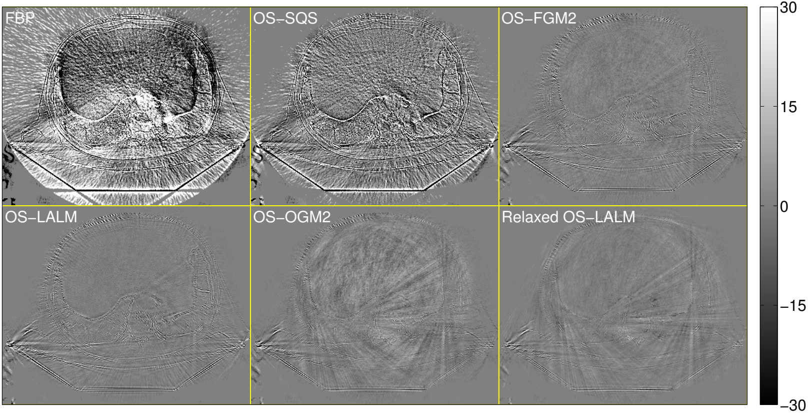

Figure: Chest: Difference images of the initial FBP image $\mathbf{x}^{(0)} - \mathbf{x}^{\star}$ and the reconstructed image $\mathbf{x}^{(5)} - \mathbf{x}^{\star}$ using OS algorithms with 20 subsets after 5 iterations.

Chest region helical scan (cont'd)

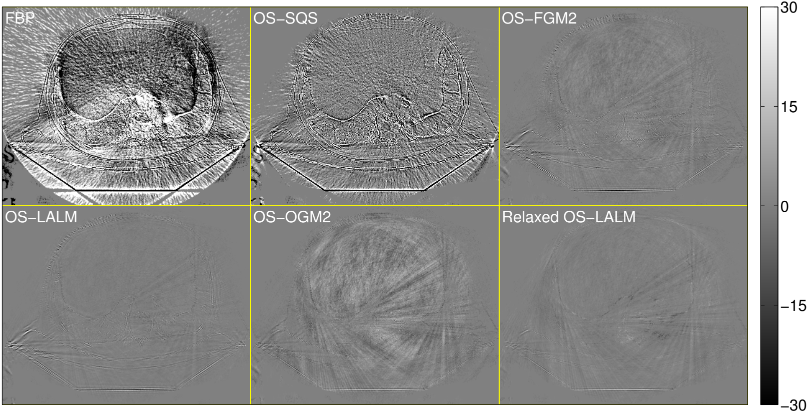

Figure: Chest: Difference images of the initial FBP image $\mathbf{x}^{(0)} - \mathbf{x}^{\star}$ and the reconstructed image $\mathbf{x}^{(10)} - \mathbf{x}^{\star}$ using OS algorithms with 20 subsets after 10 iterations.

Chest region helical scan (cont'd)

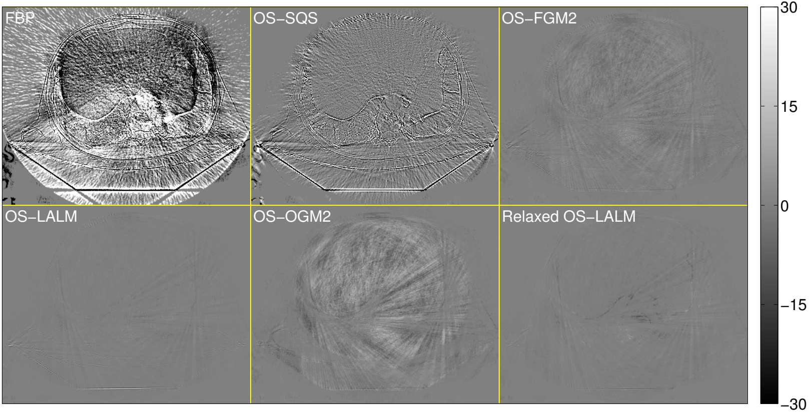

Figure: Chest: Difference images of the initial FBP image $\mathbf{x}^{(0)} - \mathbf{x}^{\star}$ and the reconstructed image $\mathbf{x}^{(20)} - \mathbf{x}^{\star}$ using OS algorithms with 20 subsets after 20 iterations. More results

Conclusions and future work

In summary,

- We proposed a relaxed variant of linearized AL methods for faster X-ray CT image reconstruction
- Experimental results showed that the proposed algorithm converges α-fold faster than its unrelaxed counterpart
- The speed-up means that one needs fewer subsets to reach an RMS difference criteria in a given number of iterations
- Empirically, the proposed algorithm is reasonably stable when we use moderate numbers of subsets

For future work,

- We want to work on the convergence rate analysis of the proposed algorithm

Conclusions and future work

In summary,

- We proposed a relaxed variant of linearized AL methods for faster X-ray CT image reconstruction
- Experimental results showed that the proposed algorithm converges α-fold faster than its unrelaxed counterpart
- The speed-up means that one needs fewer subsets to reach an RMS difference criteria in a given number of iterations
- Empirically, the proposed algorithm is reasonably stable when we use moderate numbers of subsets

For future work,

- We want to work on the convergence rate analysis of the proposed algorithm

Conclusions and future work

In summary,

- We proposed a relaxed variant of linearized AL methods for faster X-ray CT image reconstruction
- Experimental results showed that the proposed algorithm converges α-fold faster than its unrelaxed counterpart
- The speed-up means that one needs fewer subsets to reach an RMS difference criteria in a given number of iterations
- Empirically, the proposed algorithm is reasonably stable when we use moderate numbers of subsets

For future work,

- We want to work on the convergence rate analysis of the proposed algorithm

Conclusions and future work

In summary,

- We proposed a relaxed variant of linearized AL methods for faster X-ray CT image reconstruction
- Experimental results showed that the proposed algorithm converges α-fold faster than its unrelaxed counterpart
- The speed-up means that one needs fewer subsets to reach an RMS difference criteria in a given number of iterations
- Empirically, the proposed algorithm is reasonably stable when we use moderate numbers of subsets

For future work,

- We want to work on the convergence rate analysis of the proposed algorithm

Conclusions and future work

In summary,

- We proposed a relaxed variant of linearized AL methods for faster X-ray CT image reconstruction
- Experimental results showed that the proposed algorithm converges α-fold faster than its unrelaxed counterpart
- The speed-up means that one needs fewer subsets to reach an RMS difference criteria in a given number of iterations
- Empirically, the proposed algorithm is reasonably stable when we use moderate numbers of subsets

For future work,

- We want to work on the convergence rate analysis of the proposed algorithm

Conclusions and future work

In summary,

- We proposed a relaxed variant of linearized AL methods for faster X-ray CT image reconstruction
- Experimental results showed that the proposed algorithm converges α-fold faster than its unrelaxed counterpart
- The speed-up means that one needs fewer subsets to reach an RMS difference criteria in a given number of iterations
- Empirically, the proposed algorithm is reasonably stable when we use moderate numbers of subsets

For future work,

- We want to work on the convergence rate analysis of the proposed algorithm

Acknowledgments

- Supported in part by NIH grant U01 EB–018753
- Equipment support from Intel Corporation
- Research support from GE Healthcare

Shoulder region helical scan

We reconstruct a $512 \times 512 \times 109$ image from an $888 \times 32 \times 7146$ helical (pitch 0.5) CT scan.

Figure: Shoulder: Cropped images of the initial FBP image $\mathbf{x}^{(0)}$ (left), the reference reconstruction $\mathbf{x}^{\star}$ (center), and the reconstructed image $\mathbf{x}^{(20)}$ using relaxed OS-LALM with 20 subsets after 20 iterations (right).

Shoulder region helical scan (cont'd)

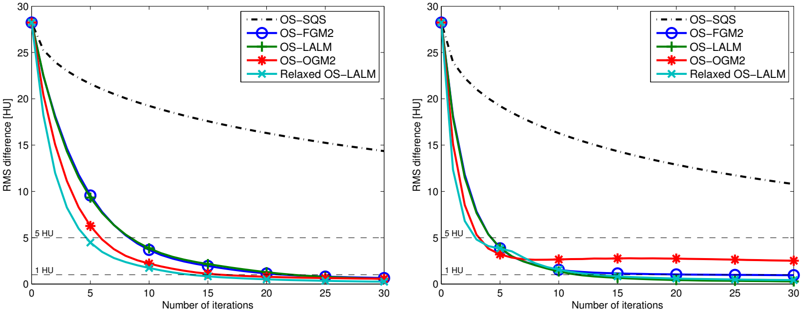

Figure: Shoulder: Convergence rate curves of different OS algorithms with 20 (left) and 40 (right) subsets.

Shoulder region helical scan (cont'd)

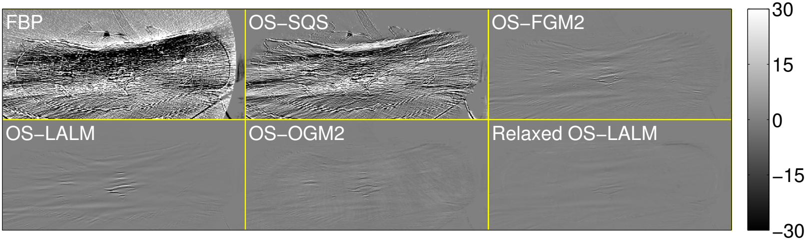

Figure: Shoulder: Difference images of the initial FBP image $\mathbf{x}^{(0)} - \mathbf{x}^{\star}$ and the reconstructed image $\mathbf{x}^{(20)} - \mathbf{x}^{\star}$ using OS algorithms with 20 subsets after 20 iterations.

Abdomen region helical scan

We reconstruct a $600 \times 600 \times 239$ image from an $888 \times 64 \times 3516$ helical (pitch 1.0) CT scan.

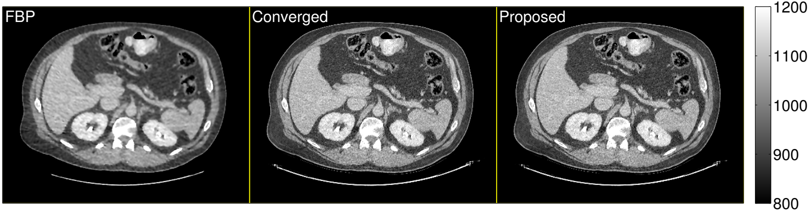

Figure: Abdomen: Cropped images of the initial FBP image $\mathbf{x}^{(0)}$ (left), the reference reconstruction $\mathbf{x}^{\star}$ (center), and the reconstructed image $\mathbf{x}^{(20)}$ using relaxed OS-LALM with 10 subsets after 20 iterations (right).

Abdomen region helical scan (cont'd)

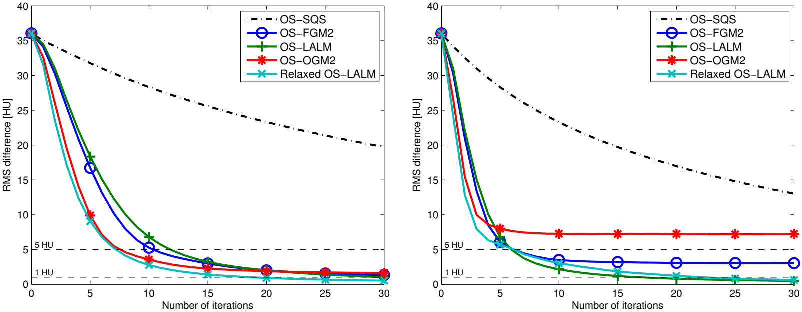

Figure: Abdomen: Convergence rate curves of different OS algorithms with 10 (left) and 20 (right) subsets.

Abdomen region helical scan (cont'd)

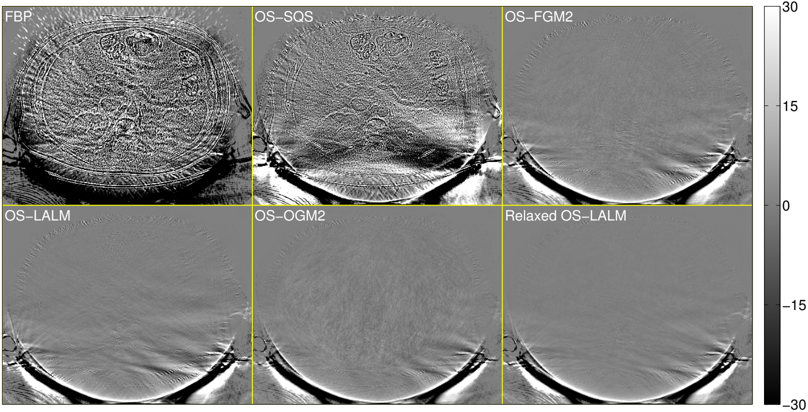

Figure: Abdomen: Difference images of the initial FBP image $\mathbf{x}^{(0)} - \mathbf{x}^\star$ and the reconstructed image $\mathbf{x}^{(20)} - \mathbf{x}^\star$ using OS algorithms with 10 subsets after 20 iterations. Conclusions and future work

Simple vs. proposed relaxed OS-LALM

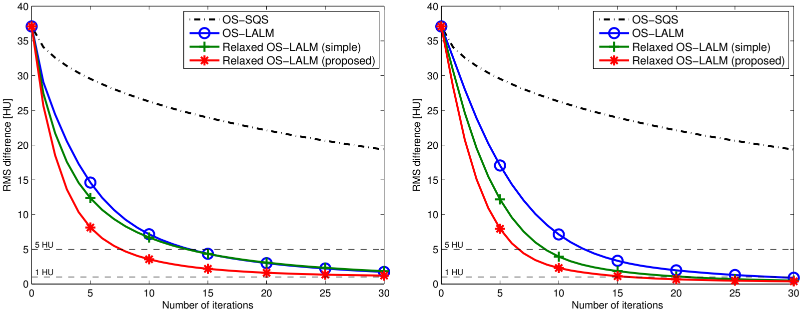

Figure: Chest: Convergence rate curves of different relaxed algorithms with a fixed AL parameter $\rho = 0.05$ (left) and the decreasing ρ (right).

Wide-cone axial scan

We reconstruct a $718 \times 718 \times 440$ image from an $888 \times 256 \times 984$ axial CT scan.

Figure: Wide-cone: Cropped images of the initial FBP image $\mathbf{x}^{(0)}$ (left), the reference reconstruction $\mathbf{x}^{\star}$ (center), and the reconstructed image $\mathbf{x}^{(20)}$ using relaxed OS-LALM with 24 subsets after 20 iterations (right).

Wide-cone axial scan (cont'd)

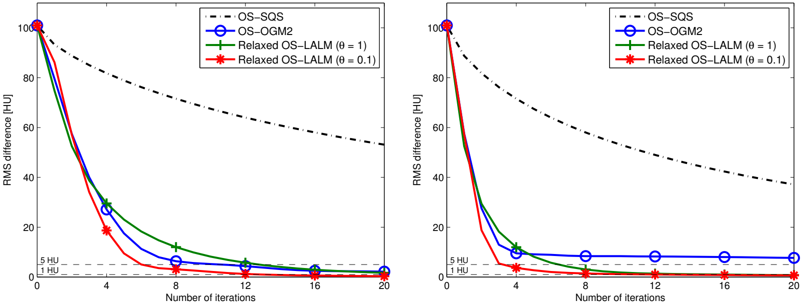

Figure: Wide-cone: Convergence rate curves of different OS algorithms with 12 (left) and 24 (right) subsets.